Strong population of excited 0^+ states in even Zr isotopes observed with the (^{14}C, ^{16}O) reaction

Wolfgang Mayer, D. Pereira,* K. E. Rehm,† H. J. Scheerer, H. J. Körner, G. Korschinek, Waltraud Mayer, and P. Sperr
Physik Department, Technische Universität München, D-8046 Garching, West Germany

Steven C. Pieper and R. D. Lawson
Argonne National Laboratory, Argonne, Illinois 60439
(Received 15 March 1982)

The two-proton pickup reaction (^{14}C, ^{16}O) on the even Mo isotopes was investigated at $E_{lab}=71$ MeV. It was found that the ratio of the ground and first excited 0^+ state cross sections changes dramatically as neutrons are added to the $N=50$ shell. While the reaction ^{92}Mo(^{14}C, ^{16}O)^{90}Zr populates the ground state three times more strongly than the first excited 0^+ state, for the heaviest isotope ^{98}Zr, the excited 0^+ state has twice the population of the ground state. Attempts to explain the cross section ratios by means of distorted-wave Born approximation calculations, based on a complete Brody-Moshinsky decomposition of the two-proton cluster and spherical shell model wave functions, were not successful.

[NUCLEAR REACTIONS ^{92,100}Mo(^{14}C,^{14}C)^{92,100}Mo, $E_{lab}=71$ MeV; measured $\sigma(\theta)$; elastic and inelastic scattering; ^{92,94,96,98,100}Mo(^{14}C, ^{16}O)^{90,92,94,96,98}Zr reactions; optical model, DWBA calculations.]

I. INTRODUCTION

Two-nucleon transfer reactions induced by light ions have been used quite extensively to obtain spectroscopic information, especially for nuclei with magic proton or neutron numbers.[1] For example, the two-neutron transfer reactions (p,t) and (t,p) on the even Zr and Sn isotopes have given valuable insight into the structure of excited 0^+ states in these nuclei. Two-proton stripping has so far been studied mainly by the (^{3}He,n) reaction. This reaction suffers however, especially at higher incident energies, from the poor energy resolution of the detected neutrons. The two-proton pickup reaction (n,^{3}He) has not been reported to our knowledge. The lightest projectile which has been used for the two-proton pickup reaction is ^{6}Li and several reports have been given for the (^{6}Li,^{8}B) reaction, mainly on 1p-shell nuclei.[2–4] Recently this reaction was used for a spectroscopic study[5] of the isotopes ^{92,96}Zr. The cross sections for the (^{6}Li,^{8}B) reactions investigated so far, however, are generally quite small. An important motivation for this study was our desire to see if the strong excitation of the excited 0^+ state at 1.59 MeV in ^{96}Zr found in the ^{100}Mo(d,^{6}Li)^{96}Zr reaction[6] would also be observed in the ^{98}Mo(^{14}C, ^{16}O)^{96}Zr reaction. Furthermore, we were interested to see if distorted-wave Born approximation (DWBA) calculations assuming a single-step cluster transfer could account for the relative strengths of the ground-state and the excited-state cross sections, or if higher order processes[7] have to be taken into account.

II. EXPERIMENTAL DETAILS

The experiments were performed at the Munich MP tandem accelerator with a 71 MeV $^{14}C^{5+}$ beam obtained from a sputter source.[8] The targets used in the experiments and their thicknesses and enrichments are summarized in Table I. The outgoing particles were momentum analyzed in a quadrupole-dipole-dipole-dipole (QDDD) magnetic

TABLE I. Thickness and isotopic purity of the targets used in these experiments. The targets were evaporated onto 5–10 μg/cm^2 C backings.

Target	Thickness (μg/cm^2)	Isotopic purity (%)
^{92}Mo	100	98.3
^{94}Mo	50	91.6
^{96}Mo	200	96.4
^{98}Mo	100	97.2
^{100}Mo	60	97.4

spectrograph and detected in the focal plane by a position-sensitive ΔE-E ionization chamber. Figure 1 shows a two-dimensional ΔE-E plot obtained for the reaction $^{14}C + {}^{96}Mo$ at 71 MeV incident energy. The magnetic field was set for the detection of the (^{14}C,$^{16}O^{8+}$) reaction. As can be seen, even weak channels can easily be separated. The energy resolution obtained in these experiments at a solid angle of 11.4 msr is between 100 and 200 keV and is mainly determined by the target thickness. In most cases, this resolution is sufficient to separate the states of interest. The normalization of the cross sections was achieved with a monitor detector positioned at $\Theta = 20°$. Absolute cross sections were obtained by a measurement of elastic scattering at forward angles where the cross section is given by its Rutherford value. For the calculation of the cross sections the 6^+, 7^+, and 8^+ charge states for the outgoing ^{16}O particles were taken into account.

III. EXPERIMENTAL RESULTS

A. Elastic and inelastic scattering

In order to obtain optical-model parameters for ^{14}C, we measured elastic and inelastic scattering of ^{14}C on ^{92}Mo and ^{100}Mo at 71 MeV incident energy. The angular distributions are shown in Figs. 2 and 3. The solid lines are optical-model (elastic) and DWBA (inelastic) calculations that are discussed in Sec. IV.

B. The (^{14}C,^{16}O) reaction

Figure 4 shows energy spectra for the reactions (^{14}C,^{16}O) on the even Mo isotopes and Fig. 5 gives the observed differential cross sections at $\theta_L = 30°$ for the ground state, 0_2^+, and 2_1^+ states of the corresponding Zr isotopes. We observe that several

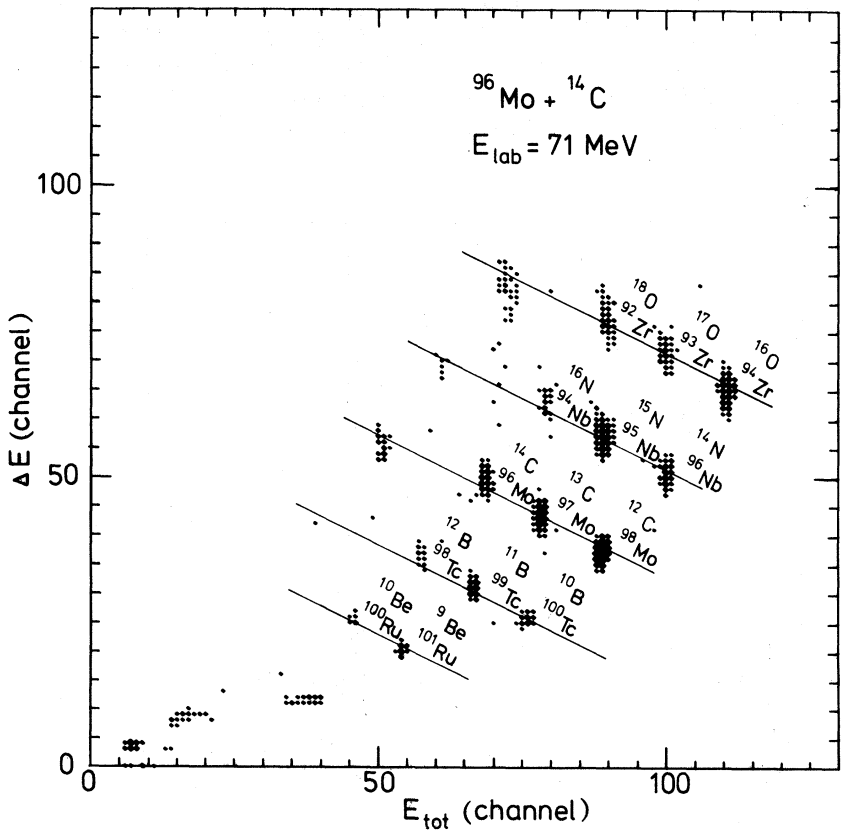

FIG. 1. Two-dimensional ΔE-E plot for the system $^{14}C + {}^{96}Mo$ at 71 MeV incident energy and a scattering angle $\Theta_{lab} = 30°$.

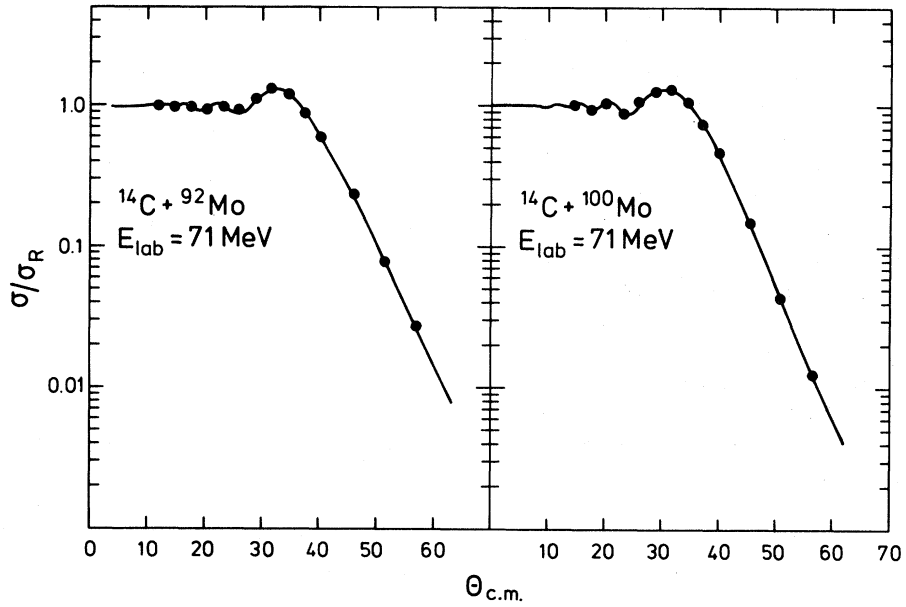

FIG. 2. Angular distributions for elastic scattering of ^{14}C on ^{92}Mo and ^{100}Mo at 71 MeV incident energy. The solid lines are optical model calculations with parameters given in Table II.

states are populated in the $^{92}Mo(^{14}C, ^{16}O)^{90}Zr$ reaction, whereas in the reaction $^{100}Mo(^{14}C,^{16}O)^{98}Zr$ mainly the two 0^+ states at 0.0 and 0.854 MeV excitation energy are excited. Furthermore, the ratio of the transition strengths between the ground state and the first excited 0^+ state in the even Zr isotopes changes in going from ^{90}Zr to ^{98}Zr. In the $^{92}Mo(^{14}C,^{16}O)^{90}Zr$ reaction the ground state is populated three times more strongly than the excited 0^+ state at 1.761 MeV excitation energy. The situation

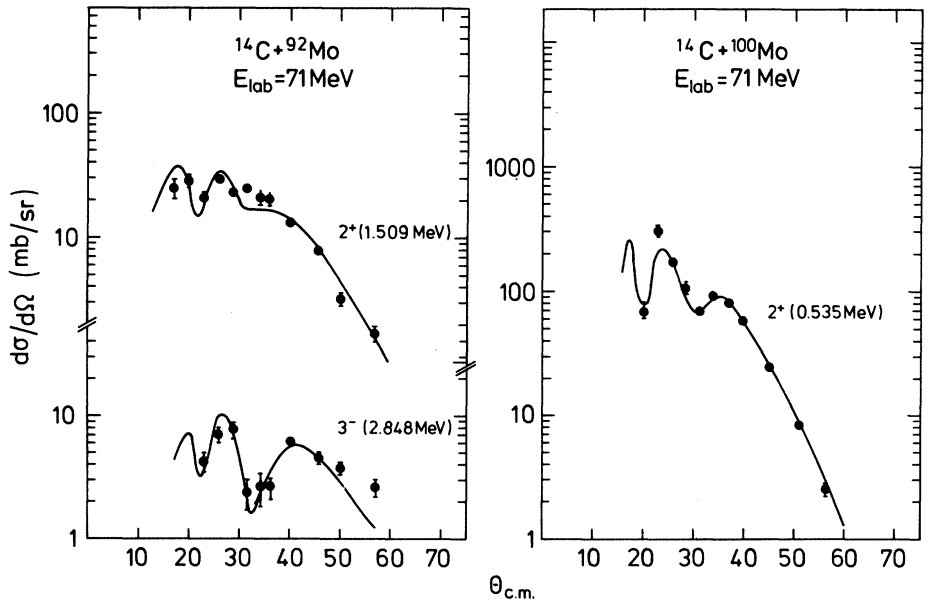

FIG. 3. Angular distributions for inelastic excitation of the 2^+ and 3^- levels at $E_x = 1.509$ and 2.848 MeV, respectively, in ^{92}Mo, and for the excitation of the 2^+ level ($E_x = 0.535$ MeV) in ^{100}Mo. The solid lines are DWBA calculations with parameters given in Tables II and III.

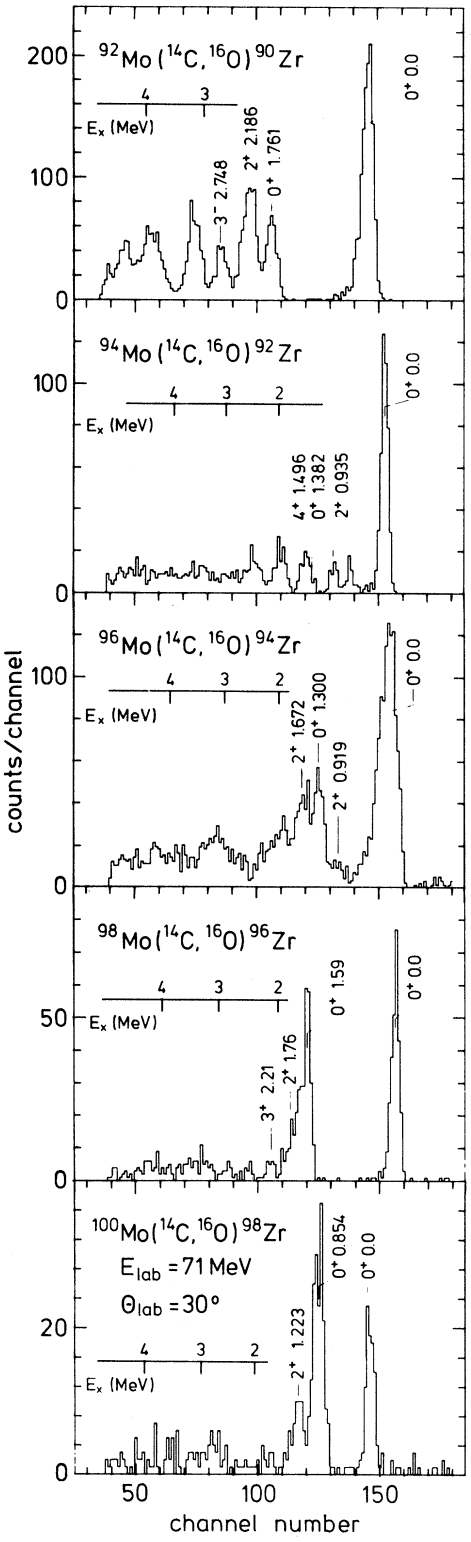

FIG. 4. Energy spectra for the reaction (^{14}C,^{16}O) on the even Mo isotopes measured at 71 MeV incident energy and $\Theta_{lab}=30°$.

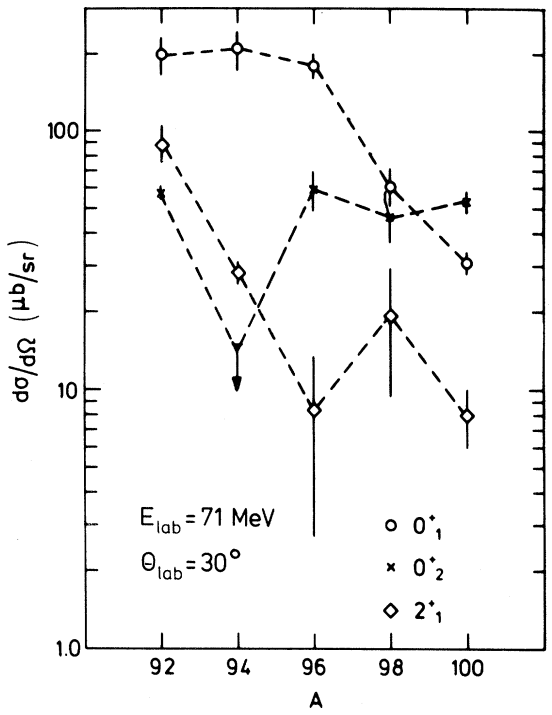

FIG. 5. Differential cross sections at $\Theta_{lab}=30°$ for the excitation of the 0^+ and first 2^+ states in the different Zr isotopes.

is reversed for the ^{100}Mo(^{14}C,^{16}O)^{98}Zr reaction, where the excited 0^+ state at 0.854 MeV energy has almost twice the transition strength of the ground state. Similar observations have been made in the (d,^{6}Li) reaction on the even Mo isotopes,[6] where the first excited 0^+ state of ^{96}Zr is strongly populated in the ^{100}Mo(d,^{6}Li)^{96}Zr reaction, while the ground state transition dominates for ^{94}Mo(d,^{6}Li)^{90}Zr. For ^{90}Zr we observe, in addition to the first two 0^+ states, mainly 2^+ and 3^- states up to an excitation energy of about 3 MeV. High spin states (6^+,8^+) could not be identified.

Owing to the higher level density, only the lowest states in ^{92}Zr could be resolved in the ^{94}Mo(^{14}C,^{16}O)^{92}Zr reaction. In addition to the strong ground state transition, the 2^+ states at 0.935, 1.847, and 2.067 MeV could be identified. The transition strength to the excited 0^+ state at $E=1.382$, which could not be completely resolved from the neighboring 4^+ state, is quite weak. The small peak at $E_x \approx 600$ keV is due to the (^{14}C,^{16}O) ground state transition on the target contaminant ^{95}Mo.

The spectrum for the reaction ^{96}Mo(^{14}C,^{16} O)^{94}Zr is still dominated by the ground state transition, while the excitation of the first excited 2^+ state at 0.919 MeV is quite weak. The multiplet at $E_x \gtrsim 1.3$

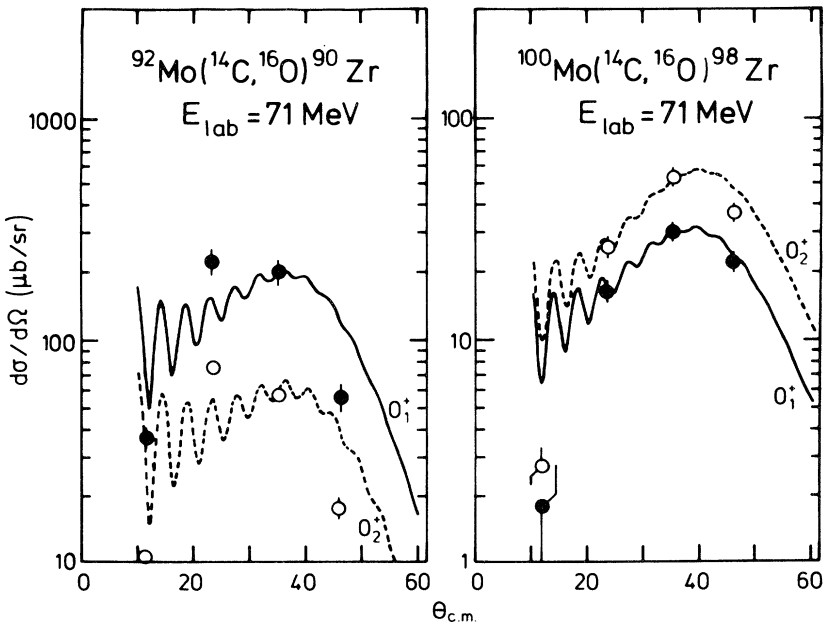

FIG. 6. Angular distributions for the excitation of the 0_1^+ (full circles) and 0_2^+ (open circles) states in the reaction ^{92,100}Mo(^{14}C,^{16}O)^{90,98}Zr at 71 MeV bombarding energy. The curves are renormalized DWBA calculations as discussed in Sec. IV.

MeV consists of the 0^+, 4^+, and 2^+ states at 1.30, 1.469, and 1.672 MeV excitation energy, respectively, which could not be completely resolved.

The energy spectrum for the reaction ^{98}Mo(^{14}C,^{16}O)^{96}Zr is already dominated by the strong transitions to the first two 0^+ states at 0.0 and 1.59 MeV excitation energy, respectively. The transitions to the 2^+ and 3^- states up to an excitation energy of 2.3 MeV are smaller by factors of 4 to 10. The energy spectrum for this reaction is similar to the one obtained in the ^{98}Mo(^{6}Li,^{8}B)^{96}Zr reaction of Ref. 5.

For the ^{100}Mo(^{14}C,^{16}O)^{98}Zr reaction the strongest transition excites the 0^+ state at 0.854 MeV in ^{98}Zr. The transition to the 2^+ state at 1.223 MeV excitation energy is four times weaker than the ground state transition. The strong population of the excited 0^+ state is unexpected because to date the 0^+ ground states have generally shown the largest transition strengths in heavy-ion induced transfer reactions.

Angular distributions for the excitation of 0^+, 2^+, and 3^- states observed in the reactions ^{92,100}Mo(^{14}C,^{16}O)^{90,98}Zr are shown in Figs. 6 and 7. They are bell shaped with a maximum of the distribution at about 30° for ^{92}Mo(^{14}C,^{16}O)^{90}Zr and about 35° for ^{100}Mo(^{14}C,^{16}O)^{98}Zr. This shift is due to a change in the ground state Q value, which decreases by 6.9 MeV in going from ^{92}Mo to ^{100}Mo. The solid lines are DWBA calculations and will be discussed in Sec. IV.

IV. DISCUSSION

A. Elastic and inelastic scattering

The optical-model analysis was performed with the program PTOLEMY.[9] The real and imaginary Woods-Saxon well depths were held fixed during the least-squares fitting procedure. The parameters so obtained are summarized in Table II. Also included are the ^{16}O + ^{92}Mo potential from Ref. 10 and a ^{16}O + ^{90}Zr potential from Ref. 11. The principal difference between the ^{14}C potentials for ^{92}Mo and ^{100}Mo is in the radius and diffuseness parameters for the imaginary potential. The DWBA calculations for inelastic scattering were also performed with the program PTOLEMY. Coulomb and nuclear excitation with equal deformation lengths were taken into account for the calculation of the form factor. The parameters used in these calculations are summarized in Table III. The agreement between theory and experiment is quite good.

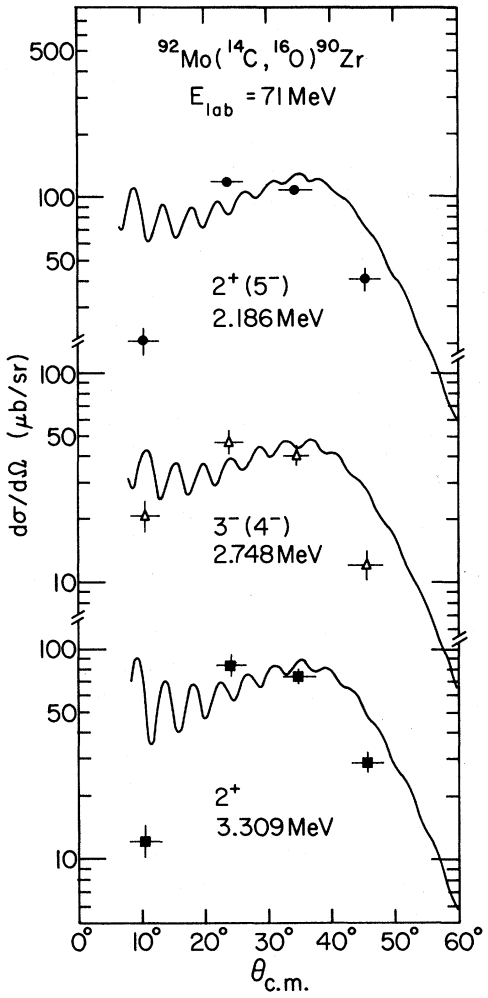

FIG. 7. Same as Fig. 5 except for excited 2^+ and 3^- states in ^{90}Zr.

B. Two-proton pickup reaction

Calculations for the (^{14}C,^{16}O) reactions were made following the procedure of Kammuri, Kubo, and Une.[12] In this method a Brody-Moshinsky decomposition is used to express the wave function of the transferred protons in terms of a relative coordinate and a cluster coordinate. The overlaps of the wave functions of the relative coordinate are computed assuming harmonic-oscillator wave functions, but bound-state wave functions corresponding to Woods-Saxon potentials that reproduce the two-proton separation energies are used for the cluster coordinates. There are several of these wave functions (with different orbital angular momentum and numbers of nodes) at each vertex. Finite-range DWBA calculations are done for all combinations of the bound-state wave functions and the resulting amplitudes are combined using the spectroscopic amplitudes to be described later. Unless otherwise stated, the finite-range DWBA calculations include the Coulomb interaction and core-core correction terms for the Coulomb and real part of the optical potential.[13]

The method just described is intermediate in computational difficulty between the traditional assumption of transfer of a cluster with internal quantum numbers $n=1$, $l=S=0$ and methods that directly use the product of Woods-Saxon bound states for the two protons.[11,14] A more detailed description of the method and a comparison with a Woods-Saxon calculation is given in the Appendix. The comparison shows that the approximate method does not give correct ratios of $(p_{1/2})^2$ and $(g_{9/2})^2$ cross sections.

In a first calculation we limited ourselves to a shell-model space in which the protons occupied $2p_{1/2}$ and $1g_{9/2}$ orbitals and the neutrons occupied $3s_{1/2}$ and $2d_{5/2}$ orbitals. The matrix elements used in these calculations were taken from fits to the energy-level data. The p-p interaction was chosen to be the "rates-fit" of Gloeckner *et al.*[15] and the $d_{5/2}$-$s_{1/2}$ single-particle splitting was taken to be 0.839 MeV.[16] This latter value was then combined with the observed spectra of ^{90}Sr and ^{90}Y to obtain as many of the (n-n) and (n-p) matrix elements as

TABLE II. Optical-model parameters for elastic scattering of ^{14}C on ^{92,100}Mo at $E_{lab}=71$ MeV, ^{16}O on ^{92}Mo at 70.7 MeV, and ^{16}O on ^{90}Zr at 80 MeV. In all cases $r_{Co}=1.2$ fm. Radii are related to radius parameters by $R=r_0(A_p^{1/2}+A_T^{1/3})$.

System	$-V$ (MeV)	r_0 (fm)	a (fm)	$-W$ (MeV)	r_{i0} (fm)	a_i (fm)
^{92}Mo + ^{14}C	100.	1.183	0.521	30.	1.065	0.712
^{100}Mo + ^{14}C	100.	1.185	0.590	30.	1.305	0.312
^{92}Mo + ^{16}O[a]	100.	1.148	0.635	20.	1.245	0.521
^{92}Zr + ^{16}O[b]	100.	1.2285	0.5155	30.	1.2044	0.5155

[a]Reference 10.
[b]Reference 11.

TABLE III. B(EL) values and deformation lengths for states in ^{92}Mo and ^{100}Mo used in the DWBA calculations.

Nucleus	ΔL	Transition energy (MeV)	B(EL) (e^2b^L)	δ_C (fm)	δ_N (fm)
^{92}Mo	2	1.509	0.113[a]	0.63	0.63
^{100}Mo	2	0.535	0.512[b]	1.28	1.28
^{92}Mo	3	2.848	0.056[c]	0.80	0.80

[a]Reference 24.
[b]Reference 25.
[c]Calculated from δ_C.

possible. Those that could not be determined from experiments were calculated using the central Schiffer-True interaction[17] with an oscillator parameter $\nu=0.213$ fm$^{-2}[\psi\sim\exp(-\nu r^2/2)]$. With these values somewhat better agreement with experiment for the excitation energies of the 0^+ and 2^+ states were obtained than if the Schiffer-True interaction had been used for all matrix elements.

The resulting spectroscopic amplitudes are listed in Table IV and the results of the corresponding DWBA calculations are given in Table V. The DWBA calculations were made with optical-potential parameters obtained by linear interpolation between the first two sets of parameters in Table II. To allow the trends of the DWBA calculations to be more easily compared with the data, the calculations have been normalized to the ^{90}Zr data by the amounts given in the table caption. The angular distributions for ^{92,100}Mo(^{14}C,^{16}O)^{90,98}Zr are shown in Fig. 6. In the figure each curve has been separately normalized to fit the data.

Both the data and the DWBA calculations exhibit decreasing ground-state cross sections as the mass of the target increases (see Table V). The decrease is due to the decrease of the ground state Q value from 9.7 MeV for ^{90}Zr to 2.9 MeV for ^{98}Zr; the optimum Q value is about 13 MeV. The presence of two valence neutrons in ^{92}Zr results in both the ^{92}Zr(0_2^+) and ^{92}Zr(2^+) states having a large neutron-excitation component since this is energetically favored. As a result the spectroscopic amplitudes for two-proton transfer are reduced and the cross sections drop from their value for ^{90}Zr. The data show the same behavior. For the heavier Mo isotopes ^{96,98,100}Mo the agreement with the DWBA calculations gets worse. According to the shell-model calculations it continues to be energetically favorable to make ^{94}Zr and ^{96}Zr 0_2^+ and 2^+ states as neutron excitations, and thus the predicted cross sections remain small. Experimentally this is not the case; the 0_2^+ cross sections are sizable for both ^{94}Zr and ^{96}Zr while the 2^+ cross section for ^{96}Zr is larger than the theoretical prediction by a factor of about 500.

In our model space, the neutrons in ^{98}Zr and ^{100}Mo again form a closed shell. Thus, the 0_2^+ and 2^+ states of ^{98}Zr must be pure proton excitations. This results in a substantial spectroscopic amplitude for the 2^+ state, in agreement with the experiment. However, due to cancellations the 0_2^+ spectroscopic amplitudes are much smaller than is required by the data.

The problem encountered in these shell model calculations might be connected to the fact that in this mass region the transition from spherical to deformed nuclear shapes occurs. While ^{96}Zr and ^{98}Mo in their ground states can still be described as spherical nuclei, the heavier isotopes ^{100}Zr and ^{102}Mo have a rotational energy spectrum.[18] The low-lying 0^+ states in the Mo and Zr isotopes are attributed to the coexistence of two different shapes, with the excited 0^+ states in ^{98,100} Mo corresponding to the deformed configuration which in ^{102}Mo becomes the ground state with a spherical 0^+ state at 0.696 MeV. The fact that the two nuclei ^{100}Mo and ^{98}Zr are in the transitional region complicates a quantitative analysis. Recent Hartree-Fock-Bogoliubov (HFB) calculations[19] have shown, however, that ^{100}Mo should have a deformed component in its ground state. Calculations for ^{98}Zr revealed[20] that

TABLE IV. Spectroscopic amplitudes for the Mo(^{14}C,^{16}O)Zr reactions. See the text for the parameters used in the shell-model calculations.

	Zr(g.s.)		Zr(0_2^+)		Zr(2^+)
	$(1g_{9/2})_0^2$	$(2p_{1/2})_0^2$	$(1g_{9/2})_0^2$	$(2p_{1/2})_0^2$	$(1g_{9/2})_2^2$
^{90}Zr	1.091	−0.489	0.096	−0.653	0.426
^{92}Zr	1.053	−0.549	0.0083	−0.540	0.177
^{94}Zr	1.059	−0.566	−0.068	−0.251	0.151
^{96}Zr	1.061	−0.553	0.125	−0.0005	0.017
^{98}Zr	1.192	−0.477	0.001	−0.239	0.627

TABLE V. Differential cross sections and cross-section ratios at $\Theta_{lab}=30°$ and $E_{lab}=71$ MeV for (^{14}C,^{16}O) reactions on the even Mo isotopes leading to the indicated states in Zr isotopes. The DWBA predictions were made with the spectroscopic amplitudes of Table IV and have been renormalized by 62.9, 580, and 1390, respectively, for the g.s., 0_2^+, and 2^+ cross sections; see text for further details.

Reaction product	$\frac{d\sigma}{d\Omega}$(g.s.)(μb/sr) Expt.	DWBA	$\frac{d\sigma}{d\Omega}(0_2^+)$($\mu$b/sr) Expt.	DWBA	$\frac{d\sigma}{d\Omega}(2^+)$($\mu$b/sr) Expt.	DWBA	$\frac{d\sigma(0_2^+)}{d\sigma(\text{g.s.})}$ Expt.	DWBA	$\frac{d\sigma(2^+)}{d\sigma(\text{g.s.})}$ Expt.	DWBA
^{90}Zr	198 ±30	198.	57 ± 3	57.	89 ±12	89.	0.29	0.29	0.45	0.45
^{92}Zr	210 ±30	164.	<13	11.	28 ± 3	13.	<0.062	0.068	0.135	0.082
^{94}Zr	179 ±20	124.	59 ±10	0.2	8.3± 3	6.4	0.33	0.002	0.046	0.052
^{96}Zr	61 ±10	90.	47 ±10	5.1	19 ± 9	0.04	0.77	0.057	0.31	0.0004
^{98}Zr	30.7± 3	39.	53.6± 5	0.3	7.8± 2	25.	1.75	0.008	0.25	0.65

the ground state in ^{98}Zr should be dominantly spherical while the excited 0^+ state at 0.854 MeV has a complicated deformed structure. The strong excitation of the excited 0^+ state in the reaction ^{100}Mo(^{14}C,^{16}O)^{98}Zr might thus be due to the good overlap between the deformed ^{100}Mo ground state and the 0_2^+ state in ^{98}Zr. Similar reasoning might explain the strong excitation of the first excited 0^+ state in the reaction ^{100}Mo(d,^{6}Li)^{96}Zr (Ref. 6).

Thus shell model calculations can only describe the trend of the cross sections in going from the reaction ^{92}Mo(^{14}C,^{16}O)^{90}Zr to ^{94}Mo(^{14}C,^{16}O)^{94}Zr. Even in these calculations the different normalization constants for the ground state and the first excited 0^+ and 2^+ states are somewhat puzzling, especially since the two 0^+ states should be closely related in their structure. In an attempt to understand these discrepancies, shell model calculations including a larger proton space (including $1g_{9/2}$, $2p_{1/2}$, $2p_{3/2}$, $1f_{5/2}$, and $2d_{5/2}$ levels) have been performed. Details of these calculations are given in the Appendix; we find that although the additional levels make sizable contributions, there is still a large disagreement with the experimental results.

In a recent study of the (^{6}Li,^{8}B) reaction leading to states in ^{92,96}Zr, Tickle *et al.*[5] reported satisfactory agreement between their DWBA calculations and data. We feel that this agreement must be fortuitous since their assumption that the relevant Mo ground states may be described as pure

TABLE VI. Spectroscopic amplitudes for the indicated reactions. For each reaction successive lines give results for various shell-model spaces as indicated by the components for which entries are given. The Schiffer-True interaction was used in seniority-0 calculations for the 0^+ states and in seniority-2 calculations for the 2^+ states.

	$(1g_{9/2})^2$	$(2p_{1/2})^2$	$2p_{3/2}2p_{1/2}$	$(2p_{3/2})^2$	$1f_{5/2}2p_{1/2}$	$1f_{5/2}2p_{3/2}$	$(1f_{5/2})^2$	$(2d_{5/2})^2$
^{92}Mo(g.s.)↔^{90}Zr(g.s.)	1.043	−0.374						
	1.094	−0.487	0.	−2.99				
	1.068	−0.432			0.		−0.243	
	1.123	−0.522	0.	−0.347	0.	0.	−0.288	
	1.127	−0.532	0.	−0.375	0.	0.	−0.305	0.149
^{92}Mo(g.s)→^{90}Zr(0_2^+)	0.085	−0.838						
	0.061	−0.683	0.	−0.234				
	0.053	−0.782			0.		−0.093	
	0.010	−0.614	0.	−0.232	0.	0.	−0.089	
	−0.000 62	−0.584	0.	−0.239	0.	0.	−0.090	0.043
^{92}Mo(g.s.)→^{90}Zr(2^+)	0.281	0.						
	0.389	0.	−0.406	−0.119				
	0.327	0.			−0.235		−0.066	
	0.427	0.	−0.341	−0.111	−0.187	−0.051	−0.063	
^{90}Zr(g.s)→^{92}Mo(2^+)	0.965	0.						
	0.916	0.	−0.010	0.				

TABLE VII. DWBA cross sections for the indicated reactions. The spectroscopic amplitudes of Table VI were used with the potentials described in the text. The cross sections and ratios are given for a c.m. scattering angle of 34.5°. For all but the first row, the cross sections were computed using all possible values of n, n', and S.

	^{92}Mo(^{14}C,^{16}O)^{90}Zr					^{90}Zr(^{16}O,^{14}C)^{92}Mo		
States used	σ(g.s.) μb/sr	$\sigma(0_2^+)$ μb/sr	$\sigma(2^+)$ μb/sr	$\sigma(0^+)/\sigma$(g.s.)	$\sigma(2^+)/\sigma$(g.s.)	σ(g.s.) μb/sr	$\sigma(2^+)$ μb/sr	$\sigma(2^+)/\sigma$(g.s.)
$1g_{9/2},2p_{1/2}$ $n=n'=1$, $l=S=0$	0.29	0.26	0.0012	0.92	0.0042	0.160	0.076	0.47
$1g_{9/2},2p_{1/2}$	2.78	0.122	0.028	0.044	0.010	1.44	1.53	1.06
$1g_{9/2},2p_{1/2},2p_{3/2}$	4.32	0.242	0.160	0.056	0.042	2.27	1.40	0.62
$1g_{9/2},2p_{1/2},1f_{5/2}$	3.32	0.105	0.072	0.032	0.022	1.73		
$1g_{9/2},2p_{1/2},2p_{3/2},1f_{5/2}$	5.29	0.189	0.224	0.036	0.042	2.79		
$1g_{9/2},2p_{1/2},2p_{3/2},1f_{5/2},2d_{5/2}$	6.77	0.237		0.035		3.58		
Experiment	198±30	57±3	89±12	0.288	0.45	220[a]	60[a]	0.27

[a]Reference 11.

$(2p_{1/2})_0^2(1g_{9/2})_0^2$ proton configuration is clearly an oversimplification. Such a description gives fractional fullness values in strong disagreement with those found in (^{3}He,d) experiments.[21] Furthermore, the assumption that the 0_2^+ states of ^{92,96}Zr are pure proton excitations is also unwarranted.

V. CONCLUSIONS

The two-proton pickup reaction (^{14}C,^{16}O) on the even Mo isotopes shows dramatic effects in both Zr(0_2^+) and Zr(2^+) production as neutrons are added outside the $N=50$ shell. Some, but not all, of the changes in the cross sections appear to be explainable by the changing possibility of describing these two excited states of Zr as neutron excitations. The ^{98}Zr(0_2^+) state is produced more strongly than the ^{98}Zr ground state; this is probably a result of the collective nature of this state. In the Appendix, the importance of a large proton shell-model space (including at least $1g_{9/2}$, $2p_{1/2}$, $2p_{3/2}$, $1f_{5/2}$, and $2d_{5/2}$ levels) has been demonstrated for two-proton transfer reactions in this mass region. Attempts to make quantitative predictions of the cross section ratios by means of DWBA calculations based on a complete Brody-Moshinsky decomposition of the two-proton cluster were not successful. A comparison with the results of Ref. 11, which uses the product of Woods-Saxon bound states, shows that the Brody-Moshinsky decomposition is unreliable in these reactions.

ACKNOWLEDGMENTS

One of us (S.C.P.) expresses his gratitude to Dr. K. E. Rehm, Professor H. J. Körner, and the rest of the E12 staff in Garching for their hospitality during his stay there. This research was supported in part by the Bundesministerium für Forschung und Technologie, Bonn, West Germany and the U. S. Department of Energy under Contract W-31-109-Eng-38.

APPENDIX

Several different shell-model descriptions of ^{90}Zr and ^{92}Mo were used for the ^{92}Mo(^{14}C,^{16}O)^{90}Zr and ^{90}Zr(^{16}O,^{14}C)^{92}Mo reactions; the latter has been studied[11] at a bombarding energy of 80 MeV. In all cases the $N=50$ neutron shell was considered to be inert. The simplest description considers the $Z=38$ proton shell to be closed and allows the two or four active protons to occupy the $1g_{9/2}$ and $2p_{1/2}$ orbitals. In addition to this, we made computations which allowed $2p_{3/2}$ and $1f_{5/2}$ holes in the $Z=38$ shell and which also allowed protons to occupy the $2d_{5/2}$ orbital. In Table VI the spectroscopic amplitudes for the various model spaces are given. The residual two-body interaction was taken to be the best-fit central Schiffer-True potential.[17] Matrix elements were calculated using harmonic-oscillator wave functions ($\sim e^{-(1/2)\nu r^2}$) with $\nu=0.213$ fm^{-2}. The single particle energies were adjusted to reproduce the observed positions of the $\frac{1}{2}^-$, $\frac{9}{2}^+$, $\frac{3}{2}^-$, $\frac{5}{2}^-$, and $\frac{5}{2}^+$ (assumed to lie at 5 MeV excitation energy) states of ^{89}Y. The $0^+\rightarrow 0^+$ spectroscopic amplitudes were computed in a seniority zero basis with all possible numbers of holes in the $p_{3/2}$ and $f_{f/2}$ levels. For the $0^+\rightarrow 2^+$ amplitudes the maximum seniority was two and at most two holes were allowed in the 2^+ levels.

The ^{14}C $\leftrightarrow$ ^{16}O vertex was described by treating

^{14}C as a superposition of $(1p_{1/2})_0^2$ and $(1p_{3/2})_0^2$ holes in ^{16}O with spectroscopic amplitudes given by the Cohen-Kurath[22] wave functions:

$$S^{1/2}(^{14}\text{C}\rightarrow{}^{16}\text{O})=0.914\ (1p_{1/2})_0^2\ ,$$
$$=0.405\ (1p_{3/2})_0^2\ .$$

The bound-state potential wells for all nuclei in this paper had $r_0=1.2$ fm, $a=0.65$ fm. In computing the overlaps of the wave functions of the relative coordinate, oscillator constants of 0.572 and 0.462 fm^{-1} were used for the projectile and target, respectively.

Table VII shows our DWBA predictions using the amplitudes of Table VI. The (^{14}C,^{16}O) calculations were made using the first optical potential in Table II, while the (^{16}O,^{14}C) calculations were made with the fourth potential. To allow comparison with the results of Ref. 11, the latter calculations were performed using only the nuclear part of the projectile bound-state potential as the effective interaction operator. Several features emerge from these two tables.

(1) The simple $2p_{1/2}$, $1g_{9/2}$ description of the protons in ^{90}Zr and ^{92}Mo is inadequate for these reactions. The spectroscopic amplitudes involving $2p_{3/2}$, $1f_{5/2}$, and $2d_{5/2}$ particles are not negligible for the 0^+ to 0^+ transitions and, in our calculations, all add coherently so that the cross sections increase by approximately 100%. As will be discussed, the DWBA method we have used does not produce results in agreement with those of Ref. 11, but we believe that this feature of the calculation is correct. The fractional fullness values for the $1g_{9/2}$, $2p_{1/2}$, $2p_{3/2}$, and $1f_{5/2}$ orbitals of ^{90}Zr and ^{92}Mo obtained from these calculations are in good agreement with light-ion measurements.[21,23]

The additional shell-model levels are even more important for the ^{90}Zr 2^+ state where the spectroscopic amplitude for $[p_{3/2}\times p_{1/2}]_2$ transfer is comparable to the $(g_{9/2})_2^2$ amplitude. This may be understood by examining the wave functions of the two states involved

$$\psi_{2^+}(^{90}\text{Zr})=A(p_{3/2})_0^4(g_{9/2})_2^2$$
$$+a[p_{3/2}^3\times p_{1/2}]_2(g_{9/2})_0^2+\cdots\ ,$$
$$\psi_{0^+}(^{92}\text{Mo})=A'(p_{3/2})_0^4(p_{1/2})_0^2(g_{9/2})_0^2$$
$$+B'(p_{3/2})_0^4(g_{9/2})_04+\cdots\ ,$$

where A, A', and B' are the large wave function components and a is a small admixture. The spectroscopic amplitude for $(g_{9/2})^2$ transfer is then $AB'/\sqrt{2}=0.389$, whereas for $[p_{3/2}\times p_{1/2}]$ transfer it is $\sqrt{5}A'a=-0.406$. Thus the geometrical factor ($\sqrt{5}$ compared to $1/\sqrt{2}$) makes this latter amplitude, which connects small and large components, comparable to the amplitude connecting large components. On the other hand, for the ^{90}Zr(0^+)$\rightarrow{}^{92}$Mo(2^+) transition, the $[p_{3/2}\times p_{1/2}]$ transfer connects a small component in the ^{90}Zr g.s. to a small component in the ^{92}Mo excited state and hence the admixed configurations have little effect.

(2) The often-made approximation that the two protons are transferred in a cluster with internal quantum numbers of only $n=1$, $l=S=0$ is clearly inadequate for these reactions. This approximation is just the first term in a sum over the complete Brody-Moshinsky decomposition of the wave functions that has been done here. As can be seen from the first two lines of Table VII, the remaining terms completely change both the magnitudes and ratios of the cross sections.

(3) The DWBA calculations for the (^{14}C,^{16}O) reactions fail to predict the experimental cross sections, despite the fairly large shell-model space used here. It is well known that two-nucleon cluster transfer calculations result in cross sections that are too small by factors of about 100. However, we had hoped that the ratios of the ^{90}Zr(0_2^+) and ^{90}Zr(2^+) cross sections to the Zr(g.s.) cross sections could be reasonably predicted. As can be seen in Table VII, these ratios are predicted to be a factor of about 10 smaller than the experimental values.

The large experimental value for the ^{90}Zr(2^+) cross section is particularly puzzling. The observed ratio to the ground-state cross section is larger than the corresponding ratio for the ^{90}Zr(^{16}O,^{14}C)^{92}Mo reaction. However, as can be seen in Table VI the spectroscopic amplitude for $(1g_{9/2})_2^2$ transfer to ^{92}Mo(2^+) is about 3.5 times that for ^{90}Zr(2^+). Furthermore, the spin factors in DWBA calculations are such that, for the same potentials, bound-state energies, and spectroscopic amplitudes, the stripping cross section will be five times greater than the pickup cross section. Thus, we would naively expect the ^{92}Mo(2^+) cross section to be some 50 times that of ^{90}Zr(2^+) and such a ratio can be seen in the second line of Table VII. In our calculations the remaining $2p_{3/2}$ and $1f_{5/2}$ amplitudes increase the ^{90}Zr(2^+) cross section by a factor of 10, leaving the cross section smaller than the ^{92}Mo(2^+) cross section by a factor of 5.

A possible explanation for this discrepancy may be that two-step processes make a very large contribution to the pickup reaction. In Ref. 11 it was found that two-step processes reduced $\sigma(2^+)/\sigma$(g.s.)

for ^{92}Mo by a factor of 2.3. However, we find that there is a very small (0.083) spectroscopic amplitude for $^{91}\mathrm{Nb}(\frac{9}{2})\rightarrow{}^{92}\mathrm{Zr}(2^+)$, and thus we doubt that two-step processes could make the required order of magnitude change for ^{90}Zr.

In an effort to understand our failure to correctly predict the ratio $\sigma(0_2^+)/\sigma(\text{g.s.})$, we attempted to reproduce the single-step results of Ref. 11 for the $^{90}\mathrm{Zr}(^{16}\mathrm{O},^{14}\mathrm{C})^{92}\mathrm{Mo}$ reaction. This calculation was made using the more exact multipole decomposition of the product of bound-state wave functions generated by a Woods-Saxon potential. We find that the approximate method used here gives a reasonable value of the $(2p_{1/2})_0^2$ component of the ^{92}Mo(g.s.) cross section, but that the $(1g_{9/2})_0^2$ component is some 20 times larger than that found in Ref. 11. Thus our cross section for the pickup reaction to ^{90}Zr(g.s.) is dominated by an overly-large $(1g_{9/2})^2$ transfer amplitude. However, as can be seen in Tables IV and VI, the $(1g_{9/2})^2$ spectroscopic amplitude to $\mathrm{Zr}(0_2^+)$ is very small; thus the $\mathrm{Zr}(0_2^+)$ cross section is dominated by the $(2p_{1/2})^2$ component and the resulting $\sigma(0_2^+)/\sigma(\text{g.s.})$ is too small.

---

*On leave of absence from Pelletron Laboratory, Sao Paulo University, Brazil.

†Present address: Argonne National Laboratory, Argonne, Illinois 60439.

[1]D. R. Bes, R. A. Broglia, O. Hansen, and O. Nathan, Phys. Lett. 34C, 1 (1977).

[2]N. A. Jelly, K. H. Wilcox, R. B. Weisenmiller, G. J. Wozniak, and J. Cerny, Phys. Rev. C 9, 2067 (1974).

[3]R. B. Weisenmiller, N. A. Jelly, D. Ashery, K. H. Wilcox, G. J. Wozniak, M. S. Zisman, and J. Cerny, Nucl. Phys. A280, 217 (1977).

[4]R. B. Weisenmiller, N. A. Jelly, K. H. Wilcox, G. J. Wozniak, and J. Cerny, Phys. Rev. C 13, 1330 (1976).

[5]R. S. Tickle, W. S. Gray, and R. D. Bent, Phys. Lett. 92B, 283 (1980).

[6]A. Saha, G. D. Jones, L. W. Put, and R. H. Siemssen, Phys. Lett. 82B, 208 (1979).

[7]D. H. Feng, T. Udagawa, and T. Tamura, Nucl. Phys. A274, 262 (1976).

[8]R. Maier, G. Korschinek, P. Spolaore, W. Kutschera, H. J. Maier, and W. Goldstein, Nucl. Instrum. Methods 155, 55 (1978).

[9]M. H. Macfarlane and S. C. Pieper, Argonne National Laboratory Report ANL-76-11, 1978 (unpublished).

[10]K. E. Rehm, H. J. Körner, M. Richter, H. P. Rother, J. P. Schiffer, and H. Spieler, Phys. Rev. C 12, 1945 (1975).

[11]P. P. Tung, K. A. Erb, M. W. Sachs, G. B. Sherwood, R. J. Ascuitto, and D. A. Bromley, Phys. Rev. C 18, 1663 (1978).

[12]T. Kammuri, K. I. Kubo, and T. Une, Z. Phys. 262, 439 (1973).

[13]R. M. DeVries, G. R. Satchler, and J. G. Cramer, Phys. Rev. Lett. 32, 1377 (1974).

[14]T. Takemasa, Phys. Lett. 55B, 28 (1975); Phys. Rev. C 18, 1677 (1978); B. F. Bayman, Phys. Rev. Lett. 32, 71 (1974).

[15]D. H. Gloeckner, M. H. Macfarlane, R. D. Lawson, and F. J. D. Serduke, Phys. Lett. 40B, 597 (1972).

[16]T. P. Cleary, Nucl. Phys. A301, 317 (1978).

[17]J. P. Schiffer and W. W. True, Rev. Mod. Phys. 48, 191 (1976).

[18]E. Cheifetz, R. C. Jared, S. G. Thompson, and J. B. Wilhelmy, Phys. Rev. Lett. 25, 38 (1970); H. Bohn, R. L. Hershberger, P. Kienle, and D. Proetel, Accelerator Laboratory, Technical University of Munich, Annual Report, 1972, p. 58.

[19]P. Federman and S. Pittel, Phys. Lett. 77B, 29 (1978).

[20]P. Federman, S. Pittel, and R. Campos, Phys. Lett. 82B, 9 (1979).

[21]H. C. Cheung, J. Kitching, J. K. P. Lee, and S. K. Mark, J. Phys. G 1, 737 (1975), and references therein.

[22]S. Cohen and D. Kurath, Nucl. Phys. A141, 145 (1970).

[23]M. R. Cates, J. B. Ball, and E. Newman, Phys. Rev. 187, 1682 (1969).

[24]P. Luksch, Nucl. Data Sheets 30, 573 (1980).

[25]P. Paradis, G. Lamoureux, R. Lecomte, and S. Manaro, Phys. Rev. C 14, 835 (1976).